Journal of Modern Optics
Vol. 58, Nos. 19–20, 10–20 November 2011, 1864–1870

Taylor & Francis
Taylor & Francis Group

Analysis of the central corneal birefringence with double-pass polarimetric images

Juan M. Bueno*

Laboratorio de Óptica, Centro de Investigación en Óptica y Nanofísica (CiOyN), Universidad de Murcia, Campus de Espinardo, 30100 Murcia, Spain

(*Received 9 November 2010; final version received 22 February 2011*)

A double-pass imaging polarimeter has been used to compute the central corneal birefringence axis and retardation in a group of 22 eyes of different ages. Sets of four retinal images corresponding to independent polarisation states in the analyser unit were recorded. From the intensities at the image central area the corneal polarimetric parameters were computed using the Stokes–Mueller formalism. Although the (slow) axis of the central cornea presented individual differences, it was mostly lying along the nasal-downward direction. Corneal retardation also presented a broad distribution. Neither the axis nor the retardation was correlated with age. There was a significant correlation between age and the intensity at the central area of the images. This technique might be a useful tool when combined with clinical instruments oriented to glaucoma detection, which include corneal compensation for polarimetric retinal imaging.

Keywords: corneal azimuth; retardation; double-pass image; polarimetry

1. Introduction

The double-pass (DP) method is a non-invasive technique used to estimate the retinal image quality [1]. However, a combination with polarimetric techniques has provided additional information on ocular polarisation properties in the living human eye [2–5]. Since different ocular structures contribute differently to the changes in the polarisation state of the light, the implementation into fundus imaging devices has been reported to improve the visualisation of retinal features, which might be of importance in clinical diagnosis [6–11].

Several imaging methods have been used to compute the *in vivo* ocular polarisation properties [2,12–15]. Whereas some of them rely on the Stokes–Mueller formalism, others have used the Jones matrix one. Mueller-matrix polarimetry has revealed ocular linear birefringence [3,12,13,16–18], which is characterised by two parameters: retardation and azimuth (or axis orientation). It is well known that the cornea, and the retina to a lesser extent, are birefringent [13,16,19–21]. In contrast, the birefringent effects of the crystalline lens are negligible [18,22]. Other polarisation properties such as diattenuation and depolarisation seem not to be as important in normal healthy eyes [5,23–25].

In particular, ocular birefringence computed from the central part of DP polarimetric images provides information on the central cornea plus the central part of the foveola (some minutes of arc) [3]. Since this part of the retina is free of nerve fibers, there is only a small contribution to the total ocular birefrigence attributed to the Henle fiber layer, what implies that most of the ocular birefringence there found is due to the cornea [21,24,26]. Since some effects of depolarisation might also take place [5,27,28], the polarimetric information extracted from DP images might be assumed to be a result of combining a linear retarder and a partial depolariser through the Mueller-matrix formalism [29,30].

Experiments in large sets of normal eyes have shown a (slow) axis for the central cornea lying along the nasally downward (ND) direction [31,32]. This agrees with other measurements with smaller sets of subjects using different techniques [3,13,30,33].

There has been an increasing interest in determining the corneal azimuth, especially in clinical environments with scanning laser polarimeters mainly oriented to glaucoma diagnosis. In particular, this is used to compensate for the corneal (or anterior segment) influence on peripapillary retardation measurements [34]. In fact, an erroneous compensation might lead to a wrong diagnosis of absence of glaucoma [35]. Commercially available setups have taken into account that retardation arising from two linear retarders (cornea and macula in the case of the eye) is subtracted

*Email: bueno@um.es

ISSN 0950–0340 print/ISSN 1362–3044 online

http://dx.doi.org/10.1080/09500340.2011.568707
http://www.tandfonline.com

or added depending on the relative angle between both retarders. A variable compensator automatically changes its azimuth and retardation to minimise or cancel the 'macular bow-tie' pattern [34–36]. More recently, Pircher and colleagues have reported a software-based technique to compensate for the corneal birefringence using polarisation sensitive optical coherence tomography (PS-OCT) [37].

In this paper, an alternative method to compute the corneal birefringence azimuth is reported based on a DP polarimetric technique. This is calculated from the Stokes vector of the light emerging from the eye, obtained from four independent polarimetric DP images.

2. Methods

2.1. Experimental setup

A schematic drawing of the DP imaging polarimeter is depicted in Figure 1. A broad description of this experimental system has been reported elsewhere [30]. A vertically polarised infrared collimated laser beam (780 nm wavelength and 1.5 mm in diameter) illuminates the eye. After double passing the ocular media and reflection at the retina, the light passes a focus corrector system (FC, used to compensate for the eye's refractive errors), is directed toward a polarisation state analyzer unit (AU) and reaches a CCD camera. AU is composed of a rotatory $\lambda/4$ plate (QWP) and a vertical linear polariser (P).

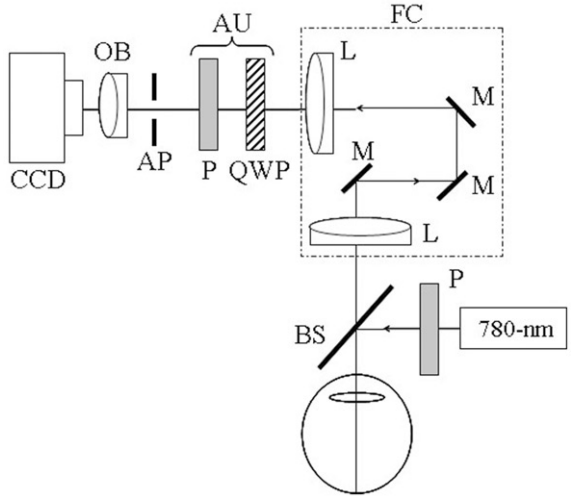

Figure 1. Sketch of the DP imaging polarimeter. P, linear polarisers; QWP, quarter-wave plate; M, mirrors; L, lenses; AP, 5 mm aperture; BS, beam splitter; OB, objective; FC, focus corrector; AU, analyser unit.

2.2. Experimental procedure

Twenty-two normal healthy subjects with ages ranging from 18 to 70 years were involved in the experiment. One eye per subject was measured (15 right and 7 left). All subjects underwent a complete ophthalmological test before the experimental session to discard any ocular pathology. All images were registered under natural accommodation for the best objective focus. This was determined while the subjects stared at the point source and FC was moved back and forward until the sharpest DP image was obtained. A bite-bar mounted on a three-axis positioning stage was used to stabilise the subject's head during measurements.

For each subject four series of five DP images (1 s exposure time, 5.5° wide-field) corresponding to independent polarisation states in AU were recorded. These states were produced by orienting the fast axis of the QWP at four angles $(-45°, 0°, 30°, 60°)$, as explained in previous literature [17,30]. For each polarisation state the five DP images were correlated and averaged. For every averaged polarimetric DP image the intensity over a circular area (2.6 arcmin in radius) around the central peak value was computed and named as I_1, I_2, I_3 and I_4. With these values the Stokes vector corresponding to the light emerging from the eye ($S_{OUT} = [S_0, S_1, S_2, S_3]^T$) was obtained as explained in [30]. Once the four elements of this vector are known, the corneal azimuth can be computed as:

$$\alpha = \frac{1}{2} a\tan\left(-\frac{DOP + S_1}{S_2}\right) \quad \text{with} \quad DOP = \frac{\sqrt{S_1^2 + S_2^2 + S_3^2}}{S_0}. \tag{1}$$

In this paper we will refer to the corneal azimuth as meaning the 'corneal birefringence slow axis', which is 90° from α [38]. Moreover, the corneal retardation (in nm) can be computed as:

$$\delta = \frac{\lambda}{360} a\cos\left(1 + \frac{2S_2}{DOP\sin(4\alpha)}\right), \tag{2}$$

where λ is the wavelength of the illumination source (780 nm in our case).

3. Results

3.1. Parameters of polarisation

Figure 2 shows the results of corneal azimuth for all subjects computed as explained in Section 2.2. Data for right and left eyes eyes are displayed as black and white symbols, respectively. We also present the corresponding mean values for both sets of eyes (triangles).

It can be observed that most azimuth values correspond to a ND direction, although they are particular for every eye. For this set of eyes values ranged between 15° nasally upward and 69° ND.

Due to the broad range of age within our subjects, we checked if there was any correlation between age and corneal birefringence parameters. Despite the decrease in retinal image quality with age [39,40], neither azimuth nor corneal retardation were correlated with age, as depicted in Figure 3. We found a wide variation in corneal retardation among the eyes involved in the present study. These ranged from 4 to 222 nm.

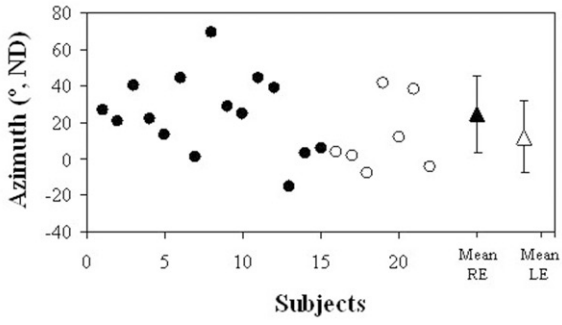

Figure 2. Central corneal azimuth for all subjects involved in this study. Black and white circles correspond to right (RE) and left (LE) eyes, respectively. Mean values (triangles) for RE and LE eyes are also included.

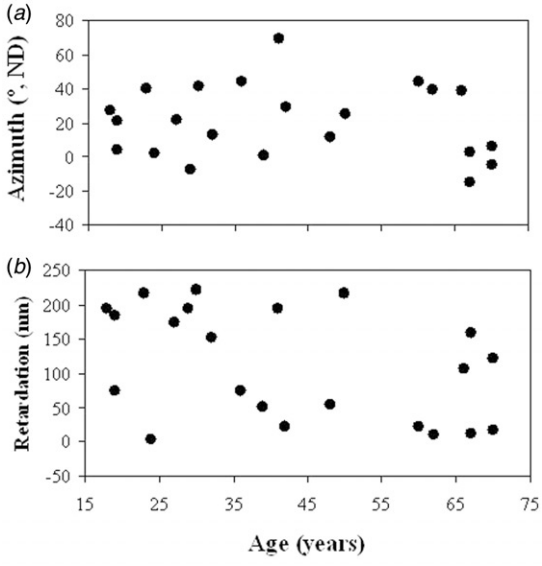

Figure 3. Values of azimuth (*a*) and retardation (*b*) for the central cornea as a function of age. No correlation was found.

3.2. *Analysis of the combined effect of image intensity, polarisation and age*

Sets of four polarimetric DP images from two different subjects (aged 18 and 60) are shown in Figure 4 as an example. Each DP image corresponds to an independent polarisation state produced in the AU.

For each subject the largest intensity value of the 4 DP images depends on the particular corneal polarisation properties [4]. This is shown in Figure 5, which plots the averaged intensity radial profiles for the images in Figure 4.

According to student paired *t*-tests, across age, no significant differences for the central intensity values were found among the different polarisation states. Across polarisation states, statistical differences were found between the subjects aged 18 and those 24 ($p = 0.02$), 32 ($p = 0.02$), 60 ($p = 0.03$) and 66 ($p = 0.03$) years old. The 48-year-old subject was also statistically different from those aged 30 and 32 (both with $p = 0.04$).

No significant relationship was found between the largest central intensity value of each set of four polarimetric DP images and the age of subjects ($p = 0.46$). The difference between the maximum and the minimum intensity was particular for each subject and not correlation with age was present ($p = 0.68$) either.

It is well known (see Figures 4 and 5) that in older eyes the core of DP images is more extended due to the increase of aberrations with age [39]. Figure 6(*a*) shows the total central intensity within a diameter of 5.2 minutes of arc for all eyes as a function of age. Each symbol corresponds to the averaged value for all DP polarimetric images. Each set of four polarimetric DP images were normalised to the highest central intensity for easier comparisons. A significant linear correlation between the amount of light and age was found ($R^2 = 0.51$; $p = 0.0002$). When taking into account the amount of light in a smaller area (2.6 arcmin in diameter), the relationship kept being significant ($R^2 = 0.43$; $p < 0.001$).

For a better understanding, Figure 6(*b*) depicts the results averaged for three groups of age (young adult, middle-aged and elderly). By considering all subjects of each age group, the intensity for the elderly group significant differed from those values for middle-aged and adult young groups ($p = 0.006$ and 0.0012, respectively). Differences between young adult and middle-age subjects were not significant ($p = 0.08$).

On the other hand, taking into account the parameters of polarisation, significant linear correlations between the azimuth and the central intensity for AU orientations of 0° ($R^2 = 0.37$; $p < 0.0002$) and −45° ($R^2 = 0.51$; $p = 0.027$) were found.

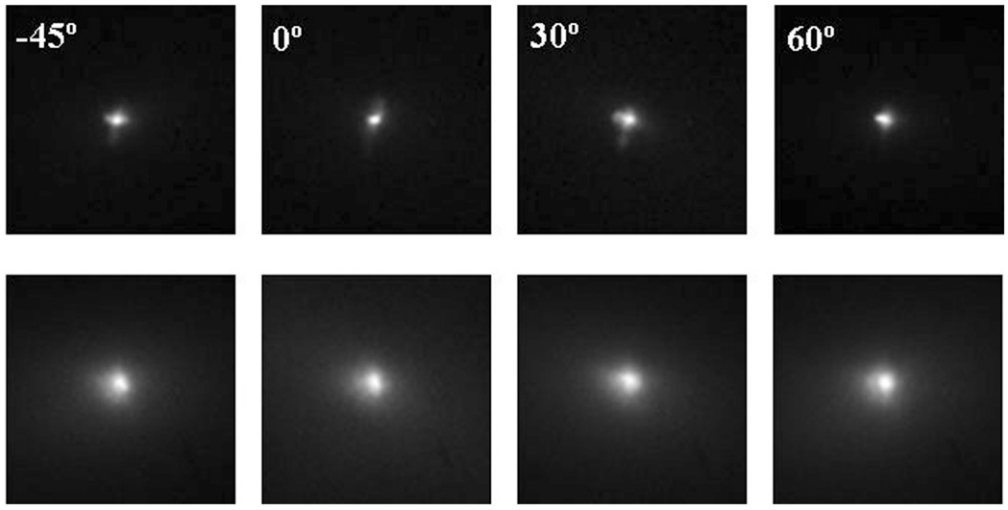

Figure 4. DP polarimetric images for two different subjects aged 18 (upper row) and 60 (bottom row). Numbers at the upper left corner indicate the orientation of the QWP axis in the AU. Each image subtends 1.5°.

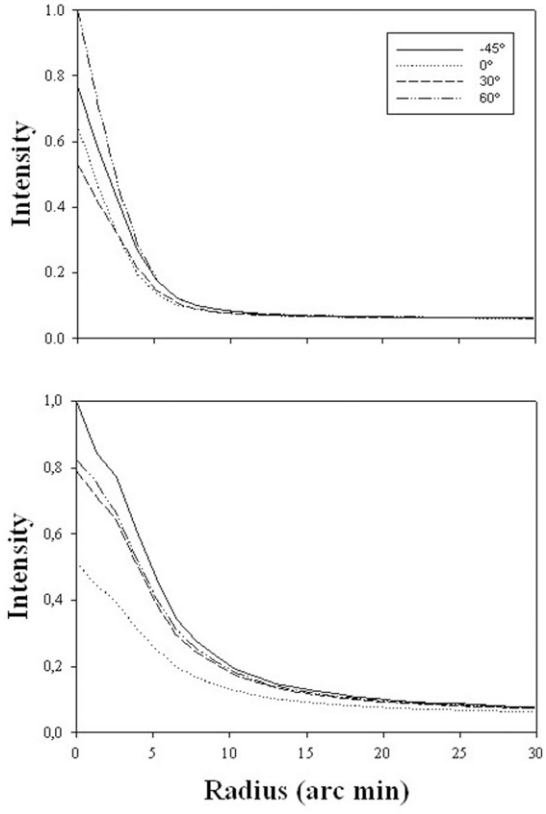

Figure 5. Normalised intensity radial profiles computed from DP images in Figure 2. For each subject the radial profiles have been normalised to the highest central intensity for a direct comparison.

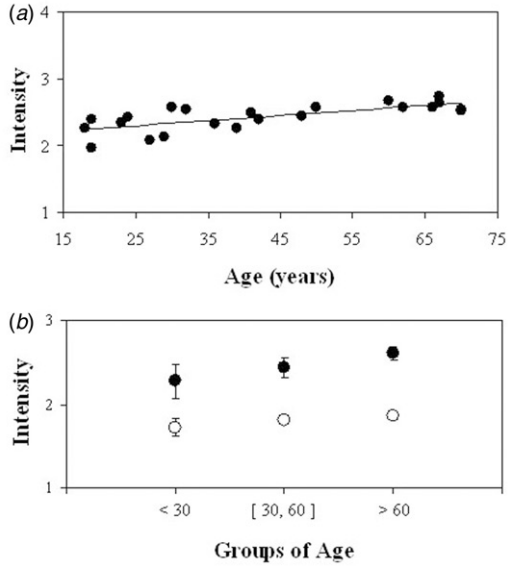

Figure 6. (*a*) Total intensity for a central area of 5.2 arcmin in the DP images for all eyes as a function of age. Each point is the average across all polarisation states. (*b*) Averaged intensity values for three groups of age for central areas of 2.6 (white circles) and 5.2 (black circles) arcmin. Age groups were chosen as young adult (<30 years, 8 subjects), middle-aged (7 subjects aged between 30 and 60 years) and elderly (>60 years, 7 subjects).

The increase in the extension of the central part of the DP image might have some influence on the calculation of the corneal azimuth. To test this, the corneal azimuth computed for a central area of 5.2 arcmin was compared to the parameter obtained when reducing the integrated area to 2.6 arcmin. Differences with the values given in Figure 2 were always smaller than 7 nm (significant linear correlation, $R^2 = 0.99$; $p < 0.0001$). This means that, at least for the reduced set of subjects here involved, corneal polarimetric parameters are correctly obtained from

DP images despite differences in the spread of the central part of the DP images among subjects.

4. Discussion

A method to calculate the azimuth and retardation of the central cornea has been proposed. This is based on DP imaging polarimetry. Keeping the incoming polarisation state fixed we measured the changes in the polarisation state of the light emerging from the eye by means of the Stokes vector. From this, the corneal polarisation parameters were computed.

In our experimental configuration the illumination laser beam travels perpendicular to the central cornea and goes to a point at the central fovea (foveola). Since the influence of the lens is much smaller than the corneal one [18] and since the retardation from the foveola can probably be neglected [21,26,37], our method assumes that most changes are due to the cornea which behaves as a linear retarder [3,12].

It has been reported that in healthy young eyes depolarisation is mainly located at the retina [5]. However, in older eyes some of these effects might be also located in the lens [18]. Moreover, the error in the computed ocular retardation increased with depolarisation [30]. To avoid this influence we also included the effects of depolarisation as a partial depolariser when computing the azimuth and the retardation (Equations (1) and (2)).

For the set of subjects involved in this study, the corneal azimuth presented individual differences, however, the preferential orientation was mainly ND (21° on average).

Different methods have been used to compute the central corneal azimuth in living human eyes. Early works reported values ranging from 0 to 40° [41,42]. Experiments using Mueller-matrix ellipsometry provided corneal azimuth values lying along the upper-temporal to lower-nasal direction, with substantial inter-individual differences [13,33]. Considerable intra-individual and inter-individual variability was also found by Greenfield and coworkers in a set of 118 eyes in 63 subjects when using a non-invasive slit lamp to observe the 4th Purkinje image through polarisation optics. However, the mean corneal azimuth was ND (51% of corneal axes lied between 10° and 30°) [31]. Later Knighton and Huang developed a corneal polarimeter (also based on Purkinje imaging) [32] and determined the central corneal azimuth in both eyes of 72 normal subjects. Their results showed again a ND tendency with a peak in the distribution between 10° and 20° (with a range between 13° nasal-upward and 72° ND). Our data agree well with these previous results. Despite the wide distribution in azimuth values here reported (Figures 2 and 3(*a*)), 55% of eyes had values between 10° and 30°.

Similarly, the retardation values also depended on the subject and our set of eyes presented a considerable wide range (Figure 3(*b*)) what is consistent with experiments reported by others authors in both large and small sets of eyes [31,32].

The present experiment corroborates that for perpendicular incidence the central cornea is accurately described as a linear retarder with its slow axis along the ND direction. Other parts of the cornea might have another type of anisotropy and although this is not the aim of this work, it is interesting to comment on this.

In 1987 van Blokland and Verhelst used Mueller-matrix polarimetry to analyse the entire cornea and found a biaxial behaviour, although the central cornea could be modelled as a linear retarder [33]. Twenty years later, Bone and Draper reported a similar anisotropy using a polarising microscope [43]. Using scanning laser polarimetry, Knighton and coworkers have recently concluded that this biaxial model mimics the corneal retardation but not accurately [44]. On the other hand, PS-OCT measurements are apparently not in agreement with the biaxial birefringence pattern [16,45]. This means that the corneal retardation model is still a subject of controversy and more studies are required. Models on multilayered systems [46], non-perpendicular incidence [16,44] and birefringence growing at corneal periphery [19] could add some light into this. Measurements with devices using perpendicular incidence and spatially resolved analysis [47,48] might also help to understand the corneal behaviour in terms of polarisation.

Within each subject the DP image intensity profiles differed among the different polarisation states (see Figure 5) as already reported by this author and his coworkers [4,25]. It was also confirmed that independently of the polarisation state, the average spread of the DP images significantly increases with age (Figure 6), what is associated with the decrease in image quality due to ocular aberrations [39]. When considering the three groups of age (Figure 6), only the central intensity for the elderly group significant differed from that corresponding to middle-aged and adult young groups.

For the sample of subjects used in this work, the corneal azimuth was linear correlated with the central intensity values corresponding to AU orientations of −45° and 0°. However, despite these well known changes with age no correlation was found for the corneal polarisation parameters (Figure 3). This fact was also tested by other authors, which supported the idea that corneal polarisation parameters are stable with age [32]. Moreover, up to a central area of 5.2 arcmin, these differences in the light distribution

between the DP images of young and older eyes did not lead to significant changes in the corneal polarimetric parameters when using different areas of integration for the calculation of the intensity.

To conclude, a simple method to compute the central corneal polarisation parameters using DP polarimetric images has been presented. As expected, considerable inter-individual variability for corneal retardation was also found. Despite differences among eyes, the azimuth was mainly pointing ND. The implementation of this method in a clinical environment might improve the existing ophthalmic imaging techniques, especially those oriented to glaucoma diagnosis.

Acknowledgements

The author thanks E. Berrio for her valuable assistance during the data collection and the early stages of the image processing, and Prof. P. Artal for helpful discussions. All the anonymous subjects included in the study are also gratefully acknowledged. The research has been supported by the Ministerio de Educación y Ciencia, Spain (Grant FIS2007-64765).

References

[1] Santamaría, J.; Artal, P.; Bescós, J. *J. Opt. Soc. Am. A* **1987,** *4,* 1109–1114.
[2] Bueno, J.M.; Artal, P. *Opt. Lett.* **1999,** *24,* 64–66.
[3] Bueno, J.M. *Vision Res.* **2000,** *40,* 3791–3799.
[4] Bueno, J.M.; Artal, P. *J. Opt. Soc. Am. A* **2001,** *18,* 489–496.
[5] Bueno, J.M. *Vision Res.* **2001,** *41,* 2687–2696.
[6] Bueno, J.M.; Campbell, M.C.W. *Opt. Lett.* **2002,** *27,* 830–832.
[7] Burns, S.A.; Elsner, A.E.; Mellem-Kairala, M.B.; Simmons, R.B. *Invest. Ophthalmol. Visual Sci.* **2003,** *44,* 4061–4068.
[8] Bueno, J.M.; Vohnsen, B. *Vision Res.* **2005,** *45,* 3526–3534.
[9] Mellem-Kairala, M.B.; Elsner, A.E.; Weber, A.; Simmons, R.B.; Burns, S.A. *Invest. Ophthalmol. Visual Sci.* **2005,** *46,* 1099–1106.
[10] Bueno, J.M.; Hunter, J.J.; Cookson, C.J.; Kisilak, M.L.; Campbell, M.C.W. *J. Opt. Soc. Am. A* **2007,** *24,* 1337–1348.
[11] Song, H.; Zhao, Y.; Qi, X.; Toco Chui, Y.; Burns, S.A. *Opt. Lett.* **2008,** *33,* 137–139.
[12] van Blokland, G.J. *J. Opt. Soc. Am. A* **1985,** *2,* 72–75.
[13] Pelz, B.C.E.; Weschenmoser, C.; Goelz, S.; Fischer, J.P.; Burk, R.O.W.; Bille, J.F. *Proc. SPIE* **1996,** *2930,* 92–101.
[14] Cense, B.; Chen, T.C.; Hyle Park, B.; Pierce, M.C.; de Boer, J.F. *Opt. Lett.* **2002,** *27,* 1610–1612.
[15] Pircher, M.; Götzinger, E.; Leitgeb, R.; Sattmann, H.; Findl, O.; Hitzenberger, C.K. *Opt. Express* **2004,** *12,* 5940–5951.
[16] Götzinger, E.; Pircher, M.; Sticker, M.; Fercher, A.; Hitzenberger, C.K. *J. Biomed. Opt.* **2004,** *9,* 94–102.
[17] Bueno, J.M.; Jaronski, J. *Ophthalmic Physiol. Opt.* **2001,** *21,* 384–392.
[18] Bueno, J.M.; Campbell, M.C.W. *Ophthalmic Physiol. Opt.* **2003,** *23,* 109–118.
[19] Bour, L.J.; Lopes Cardozo, N.J. *Vision Res.* **1981,** *21,* 1413–1421.
[20] Dreher, A.W.; Reiter, K.; Weinreb, R.N. *Appl. Opt.* **1992,** *31,* 3730–3735.
[21] klein Brink, H.B.; van Blokland, G.J. *J. Opt. Soc. Am. A* **1988,** *5,* 49–57.
[22] klein Brink, H.B. *J. Opt. Soc. Am. A* **1991,** *8,* 1788–1793.
[23] Bueno, J.M.; Artal, P. *J. Mod. Opt.* **2008,** *55,* 849–859.
[24] Twietmeyer, K.M.; Chipman, R.A.; Elsner, A.E.; Zhao, Y.; VanNasdale, D. *Opt. Express* **2008,** *16,* 21339–21354.
[25] Bueno, J.M.; Pérez, G.M. *Vision Res.* **2010,** *50,* 2439–2444.
[26] Elsner, A.E.; Weber, A.; Cheney, M.C.; VanNasdale, D.A. *Vision Res.* **2008,** *48,* 2578–2585.
[27] Baumann, B.; Götzinger, E.; Pircher, M.; Hitzenberger, C.K. *J. Biophoton.* **2009,** *2,* 426–434.
[28] Bueno, J.M.; Cookson, C.J.; Hunter, J.J.; Kisilak, M.L.; Campbell, M.C.W. *Ophthalmic Physiol. Opt.* **2009,** *29,* 247–255.
[29] Lu, S.; Chipman, R.A. *J. Opt. Soc. Am. A* **1996,** *13,* 1106–1113.
[30] Bueno, J.M. *J. Opt. A: Pure Appl. Opt.* **2004,** *6,* S91–S99.
[31] Greenfield, D.S.; Knighton, R.W.; Huang, X.-R. *Am. J. Ophthalmol.* **2000,** *129,* 715–722.
[32] Knighton, R.W.; Huang, X.-R. *Invest. Ophthalmol. Visual Sci.* **2002,** *43,* 82–86.
[33] van Blokland, G.J.; Verhelst, S.C. *J. Opt. Soc. Am. A* **1987,** *4,* 82–90.
[34] Zhou, Q.; Weinreb, R.N. *Invest. Ophthalmol. Visual Sci.* **2002,** *43,* 2221–2228.
[35] Greenfield, D.S.; Knighton, R.W.; Feuer, W.J.; Schiffman, J.C.; Zangwill, L.; Weinreb, R.N. *Am. J. Ophthalmol.* **2002,** *134,* 27–33.
[36] Weinreb, R.N.; Bowd, C.; Zangwill, L. *J. Glaucoma* **2002,** *11,* 378–384.
[37] Pircher, M.; Götzinger, E.; Baumann, B.; Hitzenberger, C.K. *J. Biomed. Opt.* **2007,** *12,* 041210.
[38] Chipman, R.A. In *Handbook of Optics*, Vol. 2; Bass, M., Ed.; McGraw-Hill: New York, 1995, Chapter 22.
[39] Guirao, A.; Gonzalez, C.; Redondo, M.; Geraghty, E.; Norrby, S.; Artal, P. *Invest. Ophthalmol. Visual Sci.* **1999,** *40,* 203–213.
[40] Brunette, I.; Bueno, J.M.; Parent, M.; Hamam, H.; Simonet, P. *Invest. Ophthalmol. Visual Sci.* **2003,** *44,* 5438–5446.
[41] Boehm, G. *Acta Ophthalmol.* **1940,** *18,* 109–169.
[42] de Vries, H.L.; Spoor, A.; Jielof, R. *Physica* **1953,** *19,* 419–432.

[43] Bone, R.A.; Draper, G. *Appl. Opt*. **2007,** *46,* 8351–8357.
[44] Knighton, R.W.; Huang, X.-R.; Cavuoto, L.A. *Opt. Express* **2008,** *16,* 13738–13751.
[45] Fanjul-Vélez, F.; Pircher, M.; Baumann, B.; Götzinger, E.; Hitzenberger, C.K.; Arce-Diego, J.L. *J. Biomed. Opt*. **2010,** *15,* 056004.
[46] Donohue, D.J.; Stoyanov, B.J.; McCally, R.L.; Farrell, R.A. *J. Opt. Soc. Am. A* **1995,** *12,* 1425–1438.
[47] Bueno, J.M.; Berrio, E.; Artal, P. *Opt. Lett*. **2003,** *28,* 1209–1211.
[48] Bueno, J.M.; Berrio, E.; Artal, P. *J. Biomed. Opt*. **2006,** *11,* 014001.